J Ginseng Res 44 (2020) 247–257

Contents lists available at ScienceDirect

Journal of Ginseng Research

journal homepage: http://www.ginsengres.org

Research Article

Ginsenoside Rg5 overcomes chemotherapeutic multidrug resistance mediated by ABCB1 transporter: *in vitro* and *in vivo* study

Sen-Ling Feng [1], Hai-Bin Luo [2], Liang Cai [1], Jie Zhang [1], Dan Wang [3], Ying-Jiang Chen [3], Huan-Xing Zhan [3], Zhi-Hong Jiang [1,4], Ying Xie [1,*]

[1] *State Key Laboratory of Quality Research in Chinese Medicine, Macau Institute for Applied Research in Medicine and Health, Macau University of Science and Technology, Macau (SAR), China*
[2] *School of Pharmaceutical Science, Sun Yat-sen University, China*
[3] *Xiamen Ginposome Pharmaceutical Co., Ltd. Xiamen, Fujian, China*
[4] *Institute of Chinese Integrative Medicine, Guangzhou Medical University, Guangzhou, China*

ARTICLE INFO

Article history:
Received 19 July 2018
Received in Revised form
28 September 2018
Accepted 31 October 2018
Available online 8 November 2018

Keywords:
ABCB1 transporter
combination therapy
ginsenoside Rg5
multidrug resistance

ABSTRACT

Background: Multidrug resistance (MDR) to chemotherapy drugs remains a major challenge in clinical cancer treatment. Here we investigated whether and how ginsenoside Rg5 overcomes the MDR mediated by ABCB1 transporter *in vitro* and *in vivo*.
Methods: Cytotoxicity and colon formation as well as the intracellular accumulation of ABCB1 substrates were carried out in MDR cancer cells A2780/T and A549/T for evaluating the reversal effects of Rg5. The expressions of ABCB1 and Nrf2/AKT pathway were determined by Western blotting. An A549/T cell xenograft model was established to investigate the MDR reversal activity of Rg5 *in vivo*.
Results: Rg5 significantly reversed ABCB1-mediated MDR by increasing the intracellular accumulation of ABCB1 substrates without altering protein expression of ABCB1. Moreover, Rg5 activated ABCB1 ATPase and reduced verapamil-stimulated ATPase activity, suggesting a high affinity of Rg5 to ABCB1 binding site which was further demonstrated by molecular docking analysis. In addition, co-treatment of Rg5 and docetaxel (TXT) suppressed the expression of Nrf2 and phosphorylation of AKT, indicating that sensitizing effect of Rg5 associated with AKT/Nrf2 pathway. In nude mice bearing A549/T tumor, Rg5 and TXT treatment significantly suppressed the growth of drug-resistant tumors without increase in toxicity when compared to TXT given alone at same dose.
Conclusion: Therefore, combination therapy of Rg5 and chemotherapy drugs is a strategy for the adjuvant chemotherapy, which encourages further pharmacokinetic and clinical studies.

1. Introduction

Although chemotherapy is one of the most effective ways for treating patients with cancer now, drug resistance leads to chemotherapy failure which is associated with the death of a great majority of patients [1]. The chemotherapy resistance induced by one drug usually are cross-resistant to multidrugs (named as multiple drug resistance, MDR) [2]. Numerous mechanisms have been explored to explain MDR, including transporter-based classical MDR mechanisms and nonclassical mechanisms which are related with alterations in the cancer cell biochemistry [3]. The classical MDR mechanisms are related to the adenosine triphosphate (ATP)-binding cassette family of membrane transporters which were overexpressed in cancer cells and pump anticancer drugs out of the cell resulting in drug concentrations below the effective concentration for therapy [4]. The first to third generations of MDR reversal agents were inhibitors of ABC transporters. Even third generation reversal agents are currently evaluated in clinical trials; however, none of them have yielded any applicable clinical results so far [5]. Therefore, finding new compounds to overcome MDR with high efficacy and low toxicity is still one of the major goals in cancer research all over the world [6,7].

Currently, researchers are stepping toward natural products for searching potential MDR antagonists based on the increasing

* Corresponding author. State Key Laboratory of Quality Research in Chinese Medicine, Macau University of Science and Technology, Macau (SAR), China.
E-mail address: yxie@must.edu.mo (Y. Xie).

https://doi.org/10.1016/j.jgr.2018.10.007
p1226-8453 e2093-4947/$ – see front matter

knowledge on their safety and efficacy [8,9]. Moreover, studies carried out recently for exploring the mechanisms of reversing MDR by natural products suggested they act on multiple targets to achieve their biological activities such as modulation of drug efflux transporters and induction of apoptosis [10,11]. Ginsenosides, also called ginseng saponins, are the major pharmacologically active ingredients of ginseng (*Panax ginseng*) with promising chemoprevention and anticancer activities. It has been demonstrated that ginsenosides could modulate the MDR [12]. For example, protopanaxadiol ginsenosides Rh2 and Rg3 from red ginseng could reverse P-glycoprotein (ABCB1, P-gp)-mediated MDR [13–15].

Ginsenoside Rg5 (Fig. 1A, $C_{42}H_{70}O_{12}$) is one of the main constituents of red ginseng and also belongs to protopanaxadiol ginsenosides [16]. It has been reported that Rg5 has antiinflammatory,

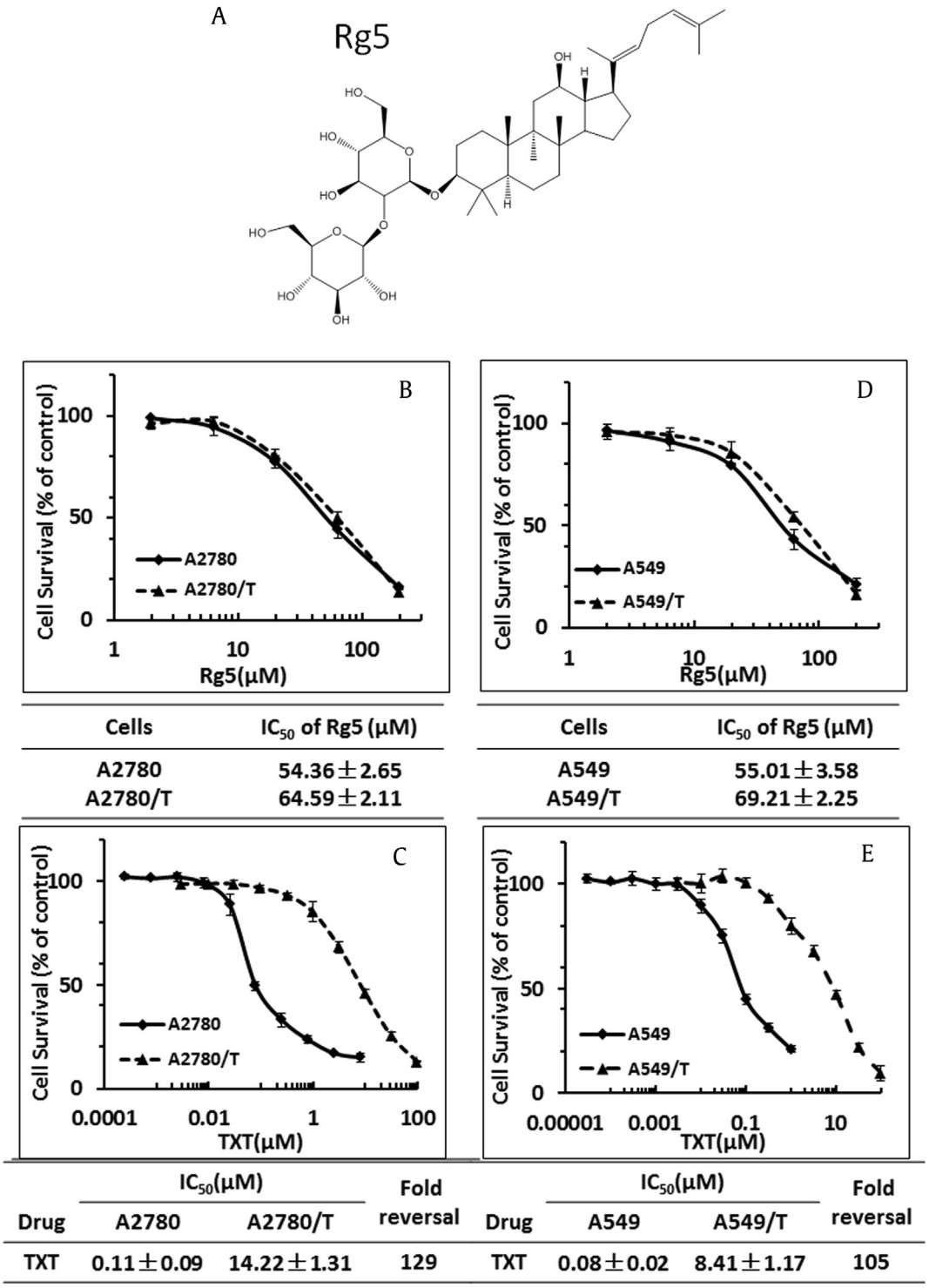

Cells	IC_{50} of Rg5 (μM)
A2780	54.36±2.65
A2780/T	64.59±2.11

Cells	IC_{50} of Rg5 (μM)
A549	55.01±3.58
A549/T	69.21±2.25

Drug	IC_{50}(μM) A2780	IC_{50}(μM) A2780/T	Fold reversal
TXT	0.11±0.09	14.22±1.31	129

Drug	IC_{50}(μM) A549	IC_{50}(μM) A549/T	Fold reversal
TXT	0.08±0.02	8.41±1.17	105

Fig. 1. Chemical structure and cytotoxicity of Rg5 in MDR cancer cells. (A) Chemical structure of Rg5. (B) Cytotoxicity of Rg5 alone in pairs of A2780/T or A2780 cells. (C) The cells were treated with various concentrations of docetaxel (TXT) for 48 hours in pairs of A2780/T or A2780 cells. (D) Cytotoxicity of Rg5 alone in pairs of A549/T or A549 cells. (E) The cells were treated with various concentrations of TXT for 48 hours in pairs of A549/T or A549 cells. Cell growth was determined using the SRB assay ($n \geq 3$).
MDR, multidrug resistance; SRB, Sulforhodamine B.

anticancer, and neuroprotective activities [17,18]. However, the reversal effect of Rg5 against the chemotherapy resistance has not been studied so far. Therefore, in this study, we investigated the effects of Rg5 in ABCB1 (P-gp)-mediated MDR at nontoxic concentrations and analyzed underlying molecular mechanisms.

2. Materials and methods

2.1. Reagents and cell culture

Rg5 was isolated and purified in our lab, and its structure and purity were confirmed by LC-MS (data were not shown). Paclitaxel (PTX), doxorubicin (DOX), docetaxel (TXT), 5-fluorouracil (5-FU), daunorubicin (DON), quinidine (QND), verapamil (Ver), propidium iodide (PI), aprotinin, leupeptin, phenyl methyl sulfonyl fluoride, and other chemicals were purchased from Sigma-Aldrich (St. Louis, MO). Extracellular signal–regulated kinases (ERK) 1/2 and actin antibodies were purchased from Santa Cruz Biotechnology; ABCB1 (P-gp) antibodies were purchased from Calbiochem, USA; Nrf2 antibodies were purchased from Abcam, Hong Kong; other antibodies such as AKT, P-AKT, and P-ERK1/2 were purchased from Cell Signaling Technology, Inc.

Human ovarian cancer cells A2780, human nonsmall cell lung cancer (NSCLC) A549 and their PTX-resistant cell line A2780/T, and A549/T were purchased from KeyGen Biotech Co., Ltd, Nanjing, China. The expression of P-gp at mRNA and protein level was confirmed in A549/T and A2780/T cells (Supplementary Fig. 1). Roswell Park Memorial Institute (RPMI)-1640 medium supplemented with 10% fetal bovine serum (GIBCO, Paisley, Scotland) was used as media for culture cancer cells at 37°C with a humidified 5% CO2 atmosphere. To maintain drug resistance, PTX (0.94μM for A2780/T and 0.24μM for A549/T) was added to the culture medium.

2.2. Cell cytotoxicity and colony formation assay

The degree of resistance was estimated by cytotoxicity using Sulforhodamine B (SRB) assay [19] and by colony formation assay [20] in human ovarian cancer cells A2780, NSCLC A549, and their PTX-resistant cell line A2780/T and A549/T (KeyGen Biotech Co., Ltd, Nanjing, China). In brief, after an incubation period, cell monolayers are fixed with 10% (wt/vol) trichloroacetic acid for 60 min, after which the excess dye is removed by washing repeatedly with 1% (vol/vol) acetic acid. The protein-bound dye (0.4% SRB) is dissolved in 10 mM tris buffer for determination at 490 nm using a plate reader (Spectra MAX 250; Molecular Devices, Sunnyvale, CA). The reversal of resistance was calculated by dividing the half maximal inhibitory concentration (IC_{50}) for cells with the drugs in the absence of Rg5 to that obtained in the presence of Rg5.

In colony formation assays, Rg5 in different concentration (containing 1.2 μM TXT) were added to A2780/T cells (1200 cells/well) in 6-well plates for 8 days. After experiments, cells were fixed with 70% ethanol and stained with crystal violet (0.5% in ethanol). The plates were rinsed with phosphate buffered saline (PBS), and the colony numbers were counted using the software of Quantity One colony counting.

2.3. Cell cycle analysis and apoptosis analysis by flow cytometry

For cell cycle analysis and apoptosis analysis, A2780/T cells were harvested after treatment, stained, and analyzed by flow cytometry as previously described [20]. Briefly, after incubation, the cells were harvested, washed with cold PBS, fixed, and permeabilized with 70% ice-cold ethanol overnight at 4°C or 2 h at −20°C. After another wash, staining solution containing PI (50μg/ml) and RNase A (200μg/ml) is incubated with cells for 1 hour in the dark. The cell cycle distribution of each sample was then determined using a flow cytometry BD FACS Aria (BD Biosciences, San Jose, CA) after pelleted, washed, and resuspended in PBS to a final concentration of 1×10^6/ml.

Apoptosis analysis were performed by double supravital staining with 5 μl recombinant fluorescein isothiocyanate–conjugated Annexin-V and 5 μl PI (50 μg/ml) for 15 min with apoptotic cells after treatment at room temperature in the dark and analyzed by flow cytometry BD FACS Aria with FlowJo software.

2.4. Drug combination assay

To evaluate the synergistic therapeutic effect between Rg5 and TXT, the Chou–Talalay methods were used according to the literature [21,22]. In brief, single drugs or premixed drug combinations were administered to A2780/T cells for 48 h. Drug dilutions in single or in combination were prepared by 2-fold serial dilutions with concentrations above or below its IC_{50} for evaluating cytotoxicity by SRB method as above description. Combination index (CI) was calculated for quantitatively defining synergism ($CI < 1$), additive ($CI = 1$), or antagonism ($CI > 1$) effect in drug combination by using CalcuSyn software v. 2.1 (Bio-soft). Moreover, synergism ($CI < 1$) include synergism ($CI = 0.3–0.7$), strong synergism ($CI = 0.1–0.3$), and very strong synergism ($CI < 0.1$).

2.5. Intracellular accumulation of DOX and Rho123

The accumulation of Rho123 (5μM) and DOX (10μM) in A2780 or A2780/T cells were measured in the absence or presence of Rg5 (2, 4, 8μM) or 20μM QND (a known ABCB1 inhibitor) as a positive control by flow cytometry analysis as described previously [20]. For fluorescent observation, cells were fixed in 4 wt% formaldehyde (Sigma-Aldrich) and stained with 1μg/mL blue-fluorescent 4′,6-diamidino-2-phenylindole (DAPI) (1 mg/mL in H2O stock solution; Invitrogen D1306) for nuclear DNA after treatment. For flow cytometry analysis, cells were then detached, resuspended in PBS after they were washed three times with cold PBS, and analyzed by flow cytometry BD FACS Aria.

2.6. Transport assay performed in Caco-2 monolayer model

For the transport assays, human colon carcinoma Caco-2 cells (ATCC) were plated in transwell at the density of 1.7 × 105/mL in 6-well plate for 21 days. The bidirection transport and efflux behavior of rhodamin123 (Rho123, 5μM) were evaluated in the Caco-2 cells in the absence or presence of Rg5 (8μM) or QND (20μM) as described previously [23]. Before and after experiments, trans-epithelial electrical resistance (WPI EVOM2 Epithelial voltohmmeter, FL, USA) was detected for evaluating the integrity of cell monolayer. At appropriate times (30, 60, 90, and 120 min), 100-μl aliquots of the apical/basolateral side were collected and replaced by fresh medium. Each sample was immediately detected for the fluorescence intensity using a microplate reader (infinite M200 PRO, TECAN, Switzerland).

2.7. ABCB1 ATPase activity assay

The impact of Rg5 on P-gp ATPase activity and the inhibitory effects of Rg5 against a Ver-stimulated ABCB1 ATPase activity were estimated with Pgp-Glo™ assay systems (Promega, USA) following manufacture's instruction [20].

2.8. Molecular docking analysis for P-gp transporter

The crystal structure of P-gp with a bound inhibitor QZ59-RRR (PDB ID 4M2S) was used for molecular docking. All the residues in P-gp were protonated at pH 7.0. Partial charges of the atoms were assigned by the Sybyl force field. The protomol which represents a set of molecular fragments to characterize the active site was generated by a ligand-based approach, and the bound ligand was utilized for protomol generation. The proto_thresh and proto_bloat parameters represent how much the protomol can be buried in the protein and how far the protomol extends outside the cavity, respectively, which were assigned by the default value 0.5 and 0. For the reliability of the molecular docking method, the bound inhibitor QZ59-RRR was redocked back to the protein with the average root-mean-square deviation (RMSD) less than 1.5 Å for the docking poses compared with the original one.

2.9. A549/T xenograft model

All animal studies were approved by the Animal Care and Use Committee at Guangzhou University of Chinese Medicine (No # ZYYL20150807). A549/T tumor bearing nude mice model was modified from A549 NSCLC xenograft models reported in the literature [24]. When the tumors grow to approximately 100 mm^3, mice were randomly divided into six groups (9-10 for each group). Saline, TXT (10 mg/kg), Rg5 (50 mg/kg), mixture of TXT (10 mg/kg) plus low dosage Rg5 (10 mg/kg), mixture of TXT (10 mg/kg) plus middle dosage Rg5 (30 mg/kg), and mixture of TXT (10 mg/kg) plus high dosage Rg5 (50 mg/kg) were intraperitoneal injection every 3 days to a total of nine injections, and tumor volume was measured every 3 days until it reached 2,000 mm^3. The animals were sacrificed on the 27th day and all tumors were immediately detached and weighed. The tumor volume was calculated using the following equation: volume $=$ (width^2 $\times$ length)/2.

2.10. Western blot analysis

Western blot was performed as preciously described [20]. Cells were washed with ice-cold PBS and were lysed in radioimmunoprecipitation assay (RIPA) buffer supplemented containing protease inhibitor mixture (1×) (Roche life Science, IN, USA). Equal amounts of proteins (30μg/lane) were resolved in 10% sodium dodecyl sulfate polyacrylamide gel electrophoresis (SDS-PAGE) and transferred onto polyvinylidene difluoride (PVDF) membranes (Millipore, Darmstadt, Germany). After blocking with 10% nonfat dry milk powder in tris-buffered saline (TBS) containing 0.1% Tween20, membranes were incubated with primary and secondary antibodies and visualized using a chemiluminescence ECL system (Super Signal West Femto, ThermoScientific). β−Actin was used as loading control.

2.11. Statistical analysis

Each experiment was repeated at least three times and presented as the mean ± standard deviation unless noted otherwise. Statistical analysis was calculated using one-way analysis of variance or Student *t* test with GraphPad Prism software, version 5.00, and the level of significance was set at a *P* value of <0.05(*), <0.01 (**), or <0.001(***).

3. Results

3.1. Rg5 reverses ABCB1-mediated MDR

The IC_{50} values of Rg5 were 64.59 and 54.36μM for resistant A2780/T cell (without adding 0.94 μM PTX to culture medium) and sensitive A2780 cell, respectively (Fig. 1B). This compound showed antitumor effects against both resistance and sensitive human ovarian and lung cancer cell lines, but its cytotoxicity is much lower than that of PTX, TXT, DOX, and etc (Fig. 1C). As Rg5 did not inhibit the growth of MDR cell lines at concentration of 8μM, therefore, the maximum concentration of Rg5 used in the reversal assays was 8 μM.

As the cytotoxicity curves shift left (Fig. 2B), treatment with Rg5 significantly enhanced the antitumor effects of TXT by decreasing the IC_{50} in a dose-dependent manner in A2780/T cells. Specifically, treatment with 2, 4, and 8 μM Rg5 reduced the IC_{50} of TXT by 1.95-, 4.55-, and 17.38-fold, respectively. However, Rg5, at tested concentrations, did not affect the IC_{50} of TXT in the sensitive A2780 cells (Fig. 2A). In addition, as shown in Table 1, Rg5 (8 μM) also sensitizing PTX, DOX, and DON to A2780/T cells with reversal fold of 6.68, 6.38, and 5.31, respectively; however, it also enhanced the effects of 5-FU (nonsubstrate of ABCB1) with a reversal fold of 6.67.

Moreover, another ABCB1-overexpressing MDR A549/T cells and its parental A549 cells were used to demonstrate the reversal effects of Rg5 to TXT and other chemotherapy drugs (Table 1). In Fig. 2C, Rg5 at dosage of 2, 4, and 8 μM significantly reduced the IC_{50} of TXT with reversal fold of 1.58, 4.47, and 11.22, respectively (Fig. 2D). Rg5 did not affect the IC_{50} of TXT in the sensitive A549 cells at same concentrations (Fig. 2C).

Colony formation assays, a gold standard for measuring the effects of cytotoxic agents on cancer cells *in vitro*, were used to evaluate the long-term reversal effects of Rg5. As expected, treatment with 1.2 μM TXT and Rg5 completely inhibited colony formation of MDR cancer cells (Fig. 2E). Either 8 μM Rg5 or 1.2 μM TXT alone did not affect the colony formation. All these results suggested that Rg5 significantly sensitized MDR cancer cells to chemotherapy drugs.

3.2. Rg5 potentiates apoptosis induced by TXT

Consistent with the results of cell growth, apoptosis was significantly enhanced by cotreatment of TXT and Rg5 as shown in Fig. 3A, while TXT (1.2 μM) or Rg5 (8 μM) alone did not induce cell apoptosis. Notably, we found that the inhibition of Rg5 at 2 μM with TXT (1.2 μM) on the cell growth is same as that of 14.22 μM TXT (IC_{50} of TXT in A2780/T) in A2780/T cells.

Since it has been recently reported that Rg5 (100 μM) induced cell cycle arrest in G0/G1 phase [25], we then evaluated whether cell cycle arrest is related to sensitizing effect of Rg5. Cell cycle progressions were examined by flow cytometry in asynchronously growing A2780/T cells and its sensitive A2780 cells treated with TXT in the absence or presence of Rg5.

There were 71.9% of cells at G1 phase and 17.1% of cells at G2 phase after incubated with 1.2μM TXT, which is similar to the phase ratios in vehicle group. Exposure to TXT (14.22μM) for 48 hours resulted in G2-M arrest (>60%) in A2780/T cells (Fig. 3B). We observed that cells treated with Rg5 and TXT (1.2μM) significantly shifted to 37.9% of G1 and 41.8% of G2 phase (Fig. 3B). This pattern was evident at 24 h after cotreatment and persisted over to 72 h. However, cell cycle distribution of A2780/T was not changed after treatment with Rg5 (8 μM) alone. Therefore, Rg5 significantly enhances the cell growth inhibition, G2M cell cycle arrest, and apoptosis induced by 1.2μM TXT, although A2780/T cells were remarkably resistant to 1.2μM TXT.

3.3. Synergistic effects of Rg5 and TXT against MDR cells

To evaluate the synergistic cytotoxic effects of Rg5 and TXT against A2780/T cells, CI based on the median-effect method were determined at 50% effective dose (ED_{50}) and 90% effective dose (ED_{90}) [22]. We found that the CI values of Rg5−TXT combination at

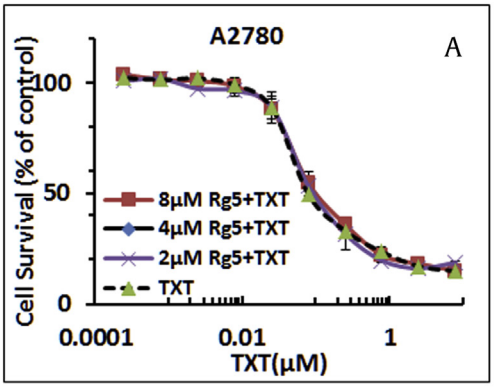

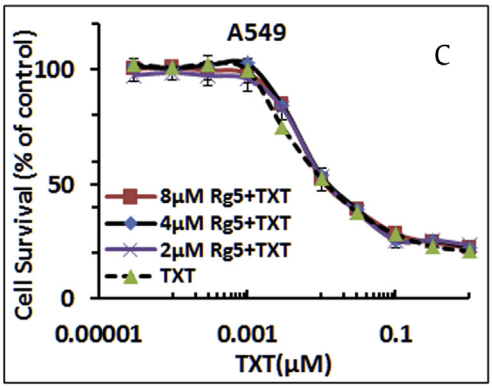

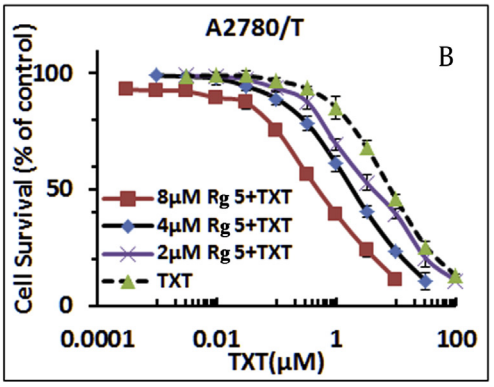

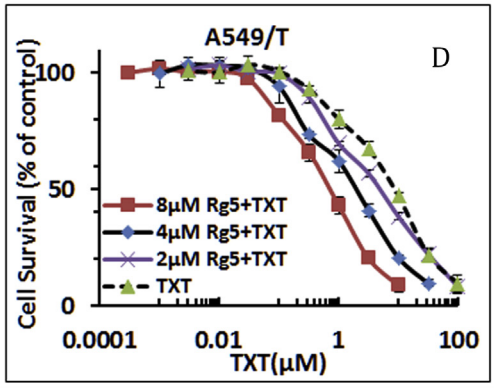

Drug	IC_{50} of TXT(μM) A2780/T	Fold reversal
TXT	14.22±1.31	1.00
+2μM Rg5	7.28±0.75*	1.95
+4μM Rg5	3.13±0.66**	4.55
+8μM Rg5	0.82±0.27***	17.38

Drug	IC_{50} of TXT(μM) A549/T	Fold reversal
TXT	8.41±1.17	1.00
+2μM Rg5	5.31±0.84	1.58
+4μM Rg5	1.88±0.76**	4.47
+8μM Rg5	0.75±0.28***	11.22

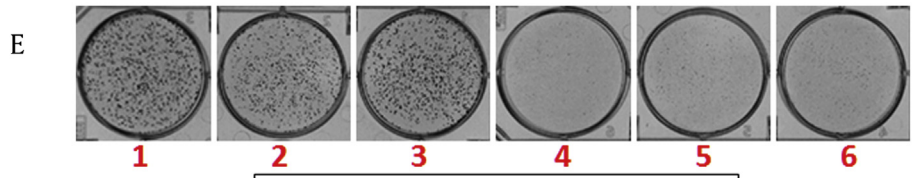

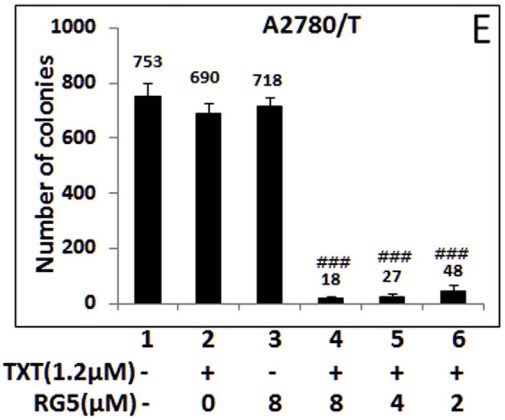

Fig. 2. Rg5 recovered sensitivity to docetaxel. Cells were treated with the indicated drugs for 48 hours and subjected to SRB assay. Rg5 reduces the IC_{50} of TXT in resistant cancer cells (A2780/T) **(B)** and A549/T **(D)** but not in drug sensitive (A2780) **(A)** and A549**(C)**. **(E)** Rg5 inhibited the colony formation of TXT in resistant cancer cells A2780/T in a dose-dependent manner. $^{\#\#},^{**}p < 0.01$, $^{\#\#\#},^{***}p < 0.001$ vs absence of Rg5.
TXT, docetaxel; SRB, Sulforhodamine B.

Table 1
Rg5 sensitized the chemotherapy Drug Paclitaxel, docetaxel, 5-fluorouracil, daunorubicin, and doxorubicin to ABCB1-Mediated Drug resistance A2780/T Cells.

Drug	A2780/T		A549/T	
	IC_{50} ± SD (μM)	Fold reversal	IC_{50} ± SD (μM)	Fold reversal
Paclitaxel	3.55 ± 0.88	1.00	3.35 ± 0.38	1.00
+2μM Rg5	1.78 ± 0.69	1.20	1.89 ± 0.27	1.78
+4μM Rg5	0.94 ± 0.45*	3.76	1.12 ± 0.35*	2.99
+8μM Rg5	0.53 ± 0.36**	6.68	0.60 ± 0.26**	5.62
Docetaxel	14.22 ± 1.31	1.00	8.41 ± 1.17	1.00
+2μM Rg5	7.28 ± 0.75*	1.95	5.31 ± 0.84	1.58
+4μM Rg5	3.13 ± 0.66**	4.55	1.88 ± 0.76**	4.47
+8μM Rg5	0.82 ± 0.27***	17.38	0.75 ± 0.28***	11.22
Doxorubicin	6.76 ± 0.79	1.00	3.58 ± 0.85	1.00
+2μM Rg5	5.62 ± 0.92	1.20	3.25 ± 1.04	1.13
+4μM Rg5	1.87 ± 0.66*	3.59	2.25 ± 0.56	1.58
+8μM Rg5	1.08 ± 0.59**	6.38	1.42 ± 0.23*	2.52
Daunorubicin	8.91 ± 0.97	1.00	6.38 ± 0.89	1.00
+2μM Rg5	6.68 ± 1.26	1.33	4.16 ± 0.59	1.35
+4μM Rg5	3.34 ± 0.83*	2.66	2.32 ± 0.72*	2.43
+8μM Rg5	1.68 ± 0.78**	5.31	0.82 ± 0.26**	6.90
5-Fluorouracil	149.87 ± 12.19	1.00	119.05 ± 9.68	1.00
+2μM Rg5	95.50 ± 7.93	1.48	94.57 ± 7.69	1.27
+4μM Rg5	42.24 ± 3.44*	3.34	59.67 ± 4.86*	1.99
+8μM Rg5	21.17 ± 1.73**	6.67	22.39 ± 2.43**	5.01

SRB, Sulforhodamine B; SD, standard deviation
Cell growth was determined using the SRB assay. The data are representative of three different experiments and are shown as mean ± SD (n = 3). $^{*}p < 0.05$, $^{**}p < 0.01$, $^{***}p < 0.001$, means significantly different from the control group in the absence of Rg5

Table 2
The values of CI and the synergism dose of Rg5 and TXT at Fa 0.5 (ED_{50}) and Fa 0.9 (ED_{90}).

	CI value	Dose Rg5(μM)	Dose TXT(μM)
Data for Fa = 0.5			
Rg5	/	69.56	/
TXT	/	/	16.02
Rg5+TXT	0.23	8.12	1.79
Data for Fa = 0.9			
Rg5	/	6.29	/
TXT	/	/	1.8
Rg5+TXT	0.05	0.18	0.04

CI, combination index; TXT, docetaxel
CI analyses of the effects of Rg5 in combination with paclitaxel are shown. The CI values were plotted as a function of the particular inhibitory effect. CI values < 1 represent a synergistic combination, CI values equal to 1 are additive and CI values > 1 represent antagonistic combinations

ED_{50} and ED_{90} were 0.23 and 0.05, indicating a strong synergistic cytotoxic effect (CI < 0.3) for Rg5–TXT combination in the A2780/T cells as shown in Table 2. With CalcuSyn simulation, the ED_{50} of Rg5 or TXT given alone is 69.56μM and 16.02 μM in A2780/T cells. But, combination with Rg5 (8.12 μM) could significantly reduce the ED_{50} of TXT to 1.79 μM which is an 8.95-fold decrease compared with TXT given alone (Table 2). The quantitative diagnostic graphics for this synergistic effect between Rg5 and TXT were shown in Supplementary Fig. 2. In addition, we evaluated the cytotoxicity of Rg5 and TXT singly or in-combination and noticed that Rg5 did not

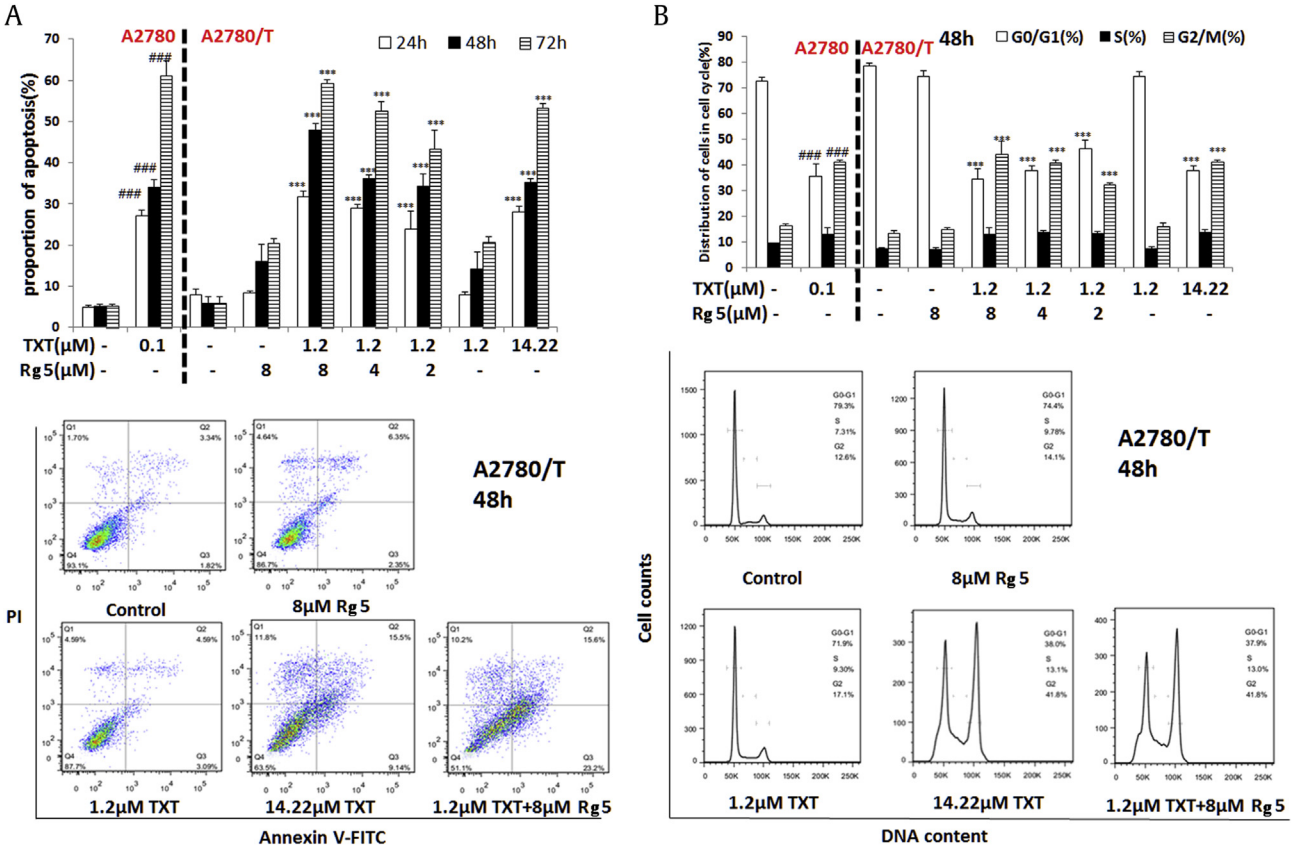

Fig. 3. Effects of Rg5 on the apoptosis and cell cycle of MDR cancer cells. (A) The cells were treated with different concentrations of Rg5 and/or TXT (1.2μM) for 48h, stained with annexin V–FITC and PI, and analyzed by flow cytometry. **(B)** The cell cycle distribution profiles of the cells treated with Rg5 and/or TXT (1.2μM) were determined by flow cytometry. The data are representative of three different experiments and are shown as mean ± SD (n = 3). $^{###}$, $^{***}p < 0.001$ vs the control group.
FITC, fluorescein isothiocyanate; MDR, multidrug resistance; PI, propidium iodide; SRB, Sulforhodamine B; SD, standard deviation; TXT, docetaxel.

affect cytotoxicity of TXT in normal lung cells BEAS-2b (Supplementary Fig. 3).

3.4. Intracellular accumulation of DOX and Rho123

To explore the underlying mechanism of this phenomenon, the intracellular accumulation of P-gp substrates such as DOX and Rho123 in sensitive A2780 cells and drug resistant A2780/T cells were performed with flow cytometry analysis.

As shown in Fig. 4, accumulation of DOX and Rho123 in A2780 indicated with fluorescence were much higher than that in A2780/T. When the drug-resistant cells were treated with 8 μM Rg5 or 20 μM QND (a reference P-gp inhibitor), the intracellular accumulation of Rho123 (Fig. 4A) and DOX (Fig. 4B) were significantly increased in A2780/T compared with vehicle control. In contrast, Rg5 did not affect the intracellular levels of DOX and Rho123 in the sensitive A2780 cells. Therefore, our results indicated that Rg5 enhanced the antitumor effects of chemotherapy agents in MDR cancer cells by significantly increasing their intracellular accumulation.

3.5. Rg5 inhibits ABCB1-mediated efflux in Caco-2 cells

To confirm the effect of Rg5 on the function of ABCB1 transporter (P-gp), Caco2 monolayer cell model which has been widely used for predicting human drug absorption and efflux activity of transporters [26] were used to evaluate the efflux ratio of the P-gp substrate Rho 123 in the presence or absence of Rg5. Notably, Rg5 increased the values of Papp (A-B) of Rho 123 (Fig. 5A) and reduced efflux ratio of Rho123 (>50%) dose dependently after 2 hours incubation (Fig. 5B). These results confirmed that Rg5 inhibited ABCB1 transporter leading to increased Rho 123 accumulations in MDR cells.

3.6. Rg5 activates the ATPase activity of ABCB1

Transporters use ATP hydrolysis to pump molecules across the membrane; therefore, we evaluated the effects of Rg5 on the ABCB1-mediated ATP hydrolysis. As shown in Fig. 5C, there is a three-fold increase over the basal activity for the ATPase activity of ABCB1 after treatment with Rg5 with EC_{50} at 9.75μM, indicating that Rg5 might interact at the drug–substrate binding site as a substrate of ABCB1.

We also examined the inhibition effects of Rg5 on Ver-stimulated ABCB1 ATPase activity for further understanding the interaction of Rg5 on the ABCB1 binding site. Ver, an ABCB1 inhibitor and substrate for transport, could competitively interfere with transportation of other ABCB1 substrates. Here, we showed Rg5 significantly reduced the ATPase activity stimulated by Ver with an IC_{50} value of 9.16μM (Fig. 5D), which suggested that Rg5 was an ABCB1 inhibitor and competitive bound to the ABCB1trasnporter.

3.7. Molecular docking analysis

To understand the binding mechanism between Rg5 and P-gp, Surflex-dock embedded in Tripos Sybyl X 2.0 was performed using the crystal structure of QZ59-RRR bound to P-gp (PDB ID: 4M2S). The selected pose of Rg5 fitted the binding site pocket of P-gp well with the docking score (Total_Score) of 5.95, which is close to that (6.01) of the reference compound QND. Our docking result indicated that Rg5 formed several kinds of specific interactions with P-gp (Fig. 6). Rg5 formed four hydrogen bonds with Tyr306, Gln721, and Tyr949 (Fig. 6B). The π-σ interaction was also observed between Rg5 and P-gp. Besides these interactions, Rg5 also formed Van der Waals interactions and hydrophobic interactions with such residues as Met68, Phe331, Phe332, Leu335, Ile336, Phe339, Gln343, Phe724, and Phe979 in the binding pocket (Fig. 6C). All these interactions contributed to the putative binding pattern of Rg5 in P-gp.

3.8. Rg5 does not affect the expression of ABCB1

Reducing ABCB1 expression or inhibiting the function of ABCB1 transporter are the most common mechanisms for the sensitizing

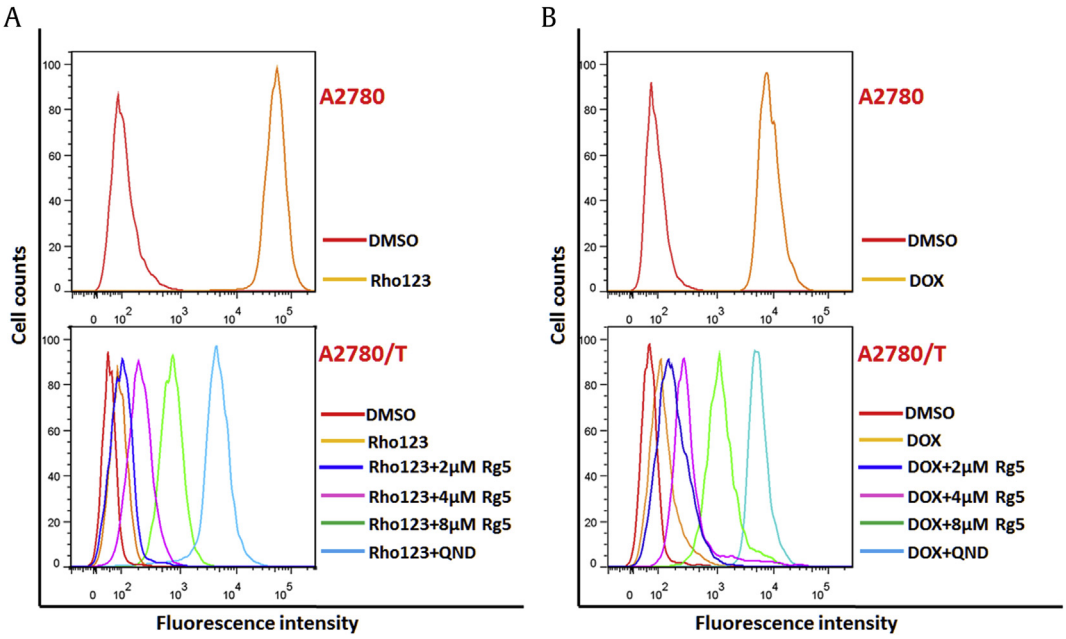

Fig. 4. Effects of Rg5 on the intracellular accumulation of Rho123 and doxorubicin (DOX) in MDR ovarian cancer cells. (A) A2780 cells or A2780/T cells treated with 5μM Rho123 for 8 hours in the absence or presence of Rg5(2,4,8μM), and 20μM quinidine (positive control) as indicated. (B) A2780 cells or A2780/T cells treated with 10μM DOX for 8 hours in the absence or presence of Rg5(2,4,8μM), and 20μM quinidine (positive control) as indicated. Intracellular DOX and Rho123 accumulation were evaluated by measuring fluorescence with flow cytometry as described in Method. The experiments were repeated for at least 3 times, presented are representative images.
DMSO, dimethyl sulfoxide; MDR, multidrug resistance; QND, quinidine.

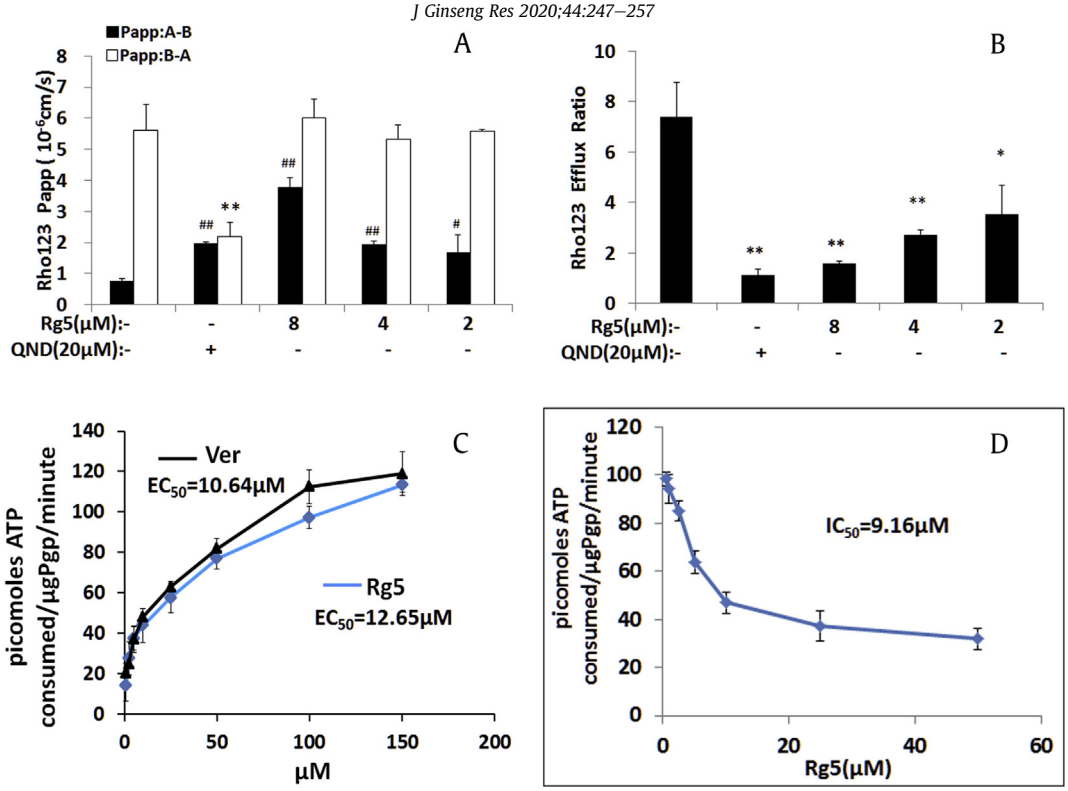

Fig. 5. Effects of Rg5 on the efflux ratio of Rho123 and DOX as well as the P-gp ATPase activity. (A) Rg5 increased the directional transport of Rho123 (5μM) and (B) decreased the efflux ratio of Rho123 (5μM) in Caco2 cells. ■AP→BL transport, □BL→AP transport. **(C)** EC_{50} measurements for stimulating the P-gp ATPase activity by Rg5 or verapamil (positive control). **(D)** IC_{50} measurements for inhibiting 200μM verapamil-stimulated P-gp ATPase activity. Luminescence was read on a luminometer, and data were analyzed as described in Material and Method. $^{\#},^{*}p < 0.05$, $^{\#\#},^{**}p < 0.01$ vs absence of Rg5.
P-gp, P-glycoprotein; DOX, doxorubicin; Ver, verampil; QND, quinidine.

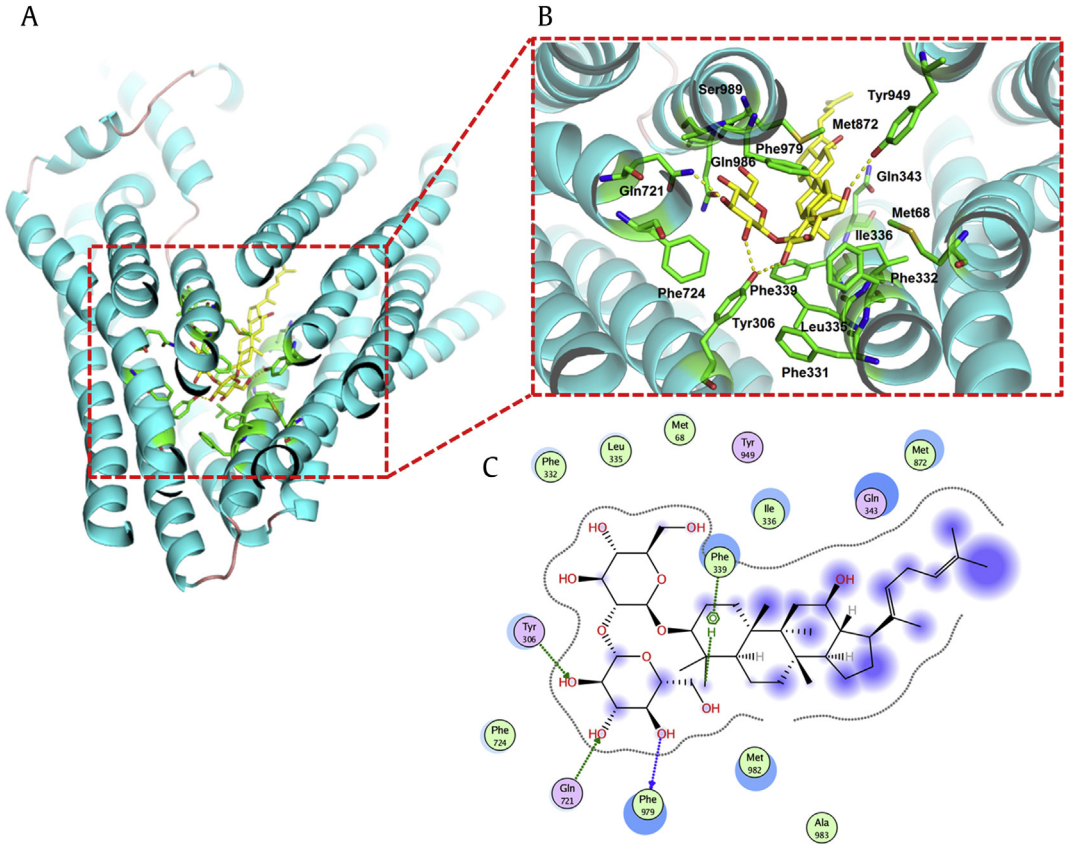

Fig. 6. Molecular docking analysis of binding pattern of Rg5 with P-gp protein. (A) Molecular docking analysis of Rg5 with P-gp. The putative binding pattern of Rg5 (yellow) and P-gp (green) is shown in the binding site. **(B)** The interactions between Rg5 and P-gp. Hydrogen bonds are depicted in dashed yellow lines. **(C)** Two-dimensional interaction mode between Rg5 and P-gp. Hydrogen bonds and π-π/σ-π interactions are shown in green and blue lines. Green and purple bubbles represent hydrophobic and polar amino acid residues, respectively.

effect on efflux transporter—mediated MDR. Here, we also evaluated the effect of Rg5 on the expression of ABCB1. Interestingly, Rg5 did not alter the protein level of ABCB1 (Fig. 7A) in A2780/T cells at the reversal concentrations. Therefore, Rg5 inhibited ABCB1 transporter function but not affect the expression of ABCB1.

3.9. Rg5 inhibits Nrf2/AKT pathways

Recently studies indicated that activation of Nrf2/PI3K/AKT, ERK pathways was closely associated with resistance to chemotherapy drugs [27,28]. Moreover, it has been reported that antitumor drugs inhibited these signaling pathways and could enhance tumor cell sensitivity to chemotherapy drugs [29,30]. Hence, we also explored the expression of total and phosphorylated AKT and ERK after treatment with Rg5. Our data indicated that phosphorylated AKT was significantly increased in A2780/T cells compared with A2780 cells. Rg5 (24μM) alone or in combination with TXT significant inhibited the expression of phosphorylated AKT, but not the expression of total AKT, ERK, and phosphorylated ERK (Fig. 7B). Therefore, inhibition of PI3K/AKT pathways was related with the enhanced cytotoxic response by combination treatment with Rg5 and TXT in ABCB1-mediated MDR cancer cells.

Moreover, it was demonstrated that blockade of transcription factor Nrf2 could sensitize a variety of cancer cells to chemotherapy drugs [31,32], indicating that the activation of Nrf2 enhances chemoresistance [33]. Here, we observed a remarkably higher level of Nrf2 in A2780/T cells than that of A2780 cells, while combination treatment of Rg5 with TXT suppressed the expression of Nrf2 (Fig. 7). These results indicated that MDR reversal effect of Rg5 to chemotherapy agents was also caused by inhibition of Nrf2/PI3K/AKT pathways.

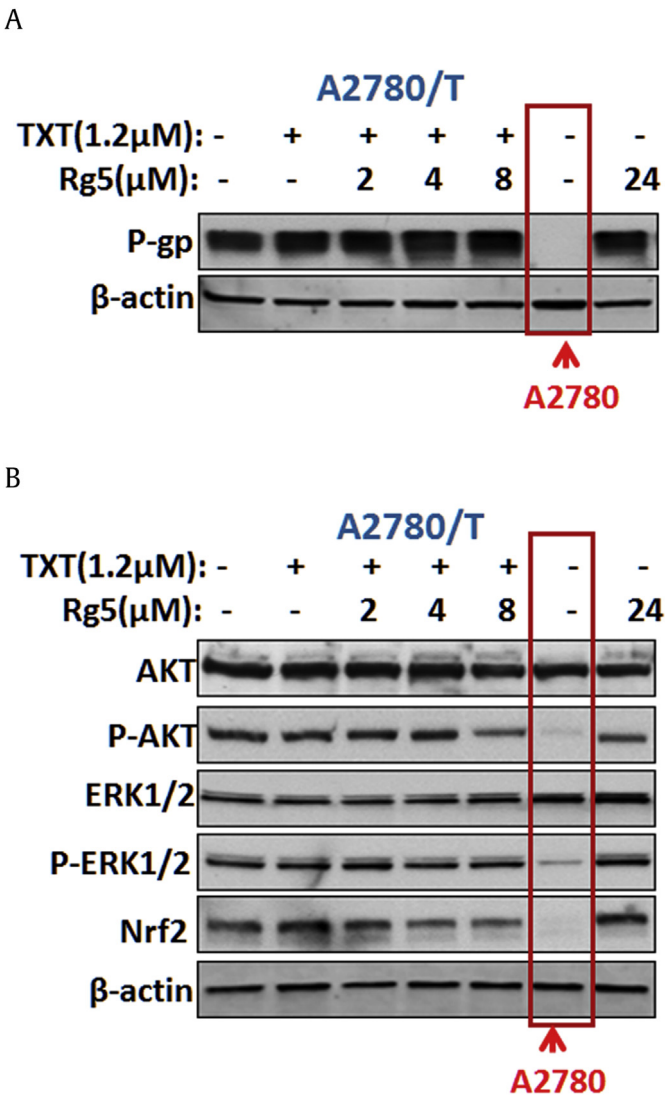

Fig. 7. Effects of the combination treatment of TXT and Rg5 on the expression of ABCB1 and AKT/ERK/Nrf2 pathway. (A) Combination treatment of TXT and Rg5 did not influence P-gp expression levels in A2780/T cells, but (B) reduced the phosphorylation of AKT and the expression level of Nrf2 which are significantly increased in A2780/T cells by compared with A2780 cells (marked with red lines).
P-gp, P-glycoprotein; TXT, docetaxel.

3.10. Rg5 overcomes TXT resistance in nude mice bearing A549/T cells tumor

We next evaluated whether Rg5 could overcome TXT resistance in A549/T xenograft model. Based on the literature, an effective dose (10 mg/kg) was chosen for the TXT [34,35], which is within the safety range and well tolerated in our study (Fig. 8A). As shown in Fig. 8B, TXT alone has no effect on treating MDR tumors at 10 mg/kg as there is similar tumor progression between TXT treated group and vehicle control group. However, treatment with both TXT and Rg5 significantly inhibited the growth of drug resistance tumor in a dose-dependent manner, indicating considerable therapeutic efficacy. Notably, high dose of Rg5 (50mg/kg) with TXT greatly diminished the growth of tumors by 48% in A549/t xenograft model.

At the end of the experiment, tumors were carefully removed and weighed (Fig. 8C—D). The smallest tumor weight was observed with the group given TXT and high dose of Rg5, which was 2.3-fold smaller than that of the vehicle group and nearly two-fold smaller than that of TXT or Rg5 treated groups. Moreover, weight loss was not observed in the combination treatment groups indicating Rg5 did not increase toxicity of TXT. All results demonstrate that combination therapy of Rg5 with TXT overcomes the ABCB1-mediated resistance *in vitro* and *in vivo*.

4. Discussion

TXT has been used as first-line chemotherapy drug since 2004, but the occurrence of resistance to TXT has been a major reason leading to the treatment failure of cancer. Currently, scientists are aimed on discovering more efficacious and less toxic compounds from natural products to reverse MDR. Pilot studies in small animal and human clinical trials indicated that Rg5 had a favorable safety profile and significant effects in reducing cisplatin-induced nephrotoxicity, antioxidant, antiapoptotic, and antiinflammatory effects as well as treating diabetes [16,36]. Although the pharmacokinetic behavior of Rg5 has not been investigated, other protopanaxadiol ginsenosides such as Rh2 and Rg3 from red ginseng have relative high plasma concentrations. For example, the average maxima concentration of Rg3 was 36.4mg/L (46.5μM) in tumor-bearing rats and 81.6 mg/L (104.2μM) in rats after oral administration at the dose of 50 mg/kg of ginsenoside Rg3 [37]. Considering its appropriate structure and safety, we investigated whether Rg5 could sensitize the ABCB1-overexpression MDR cancer cells to chemotherapy agents *in vitro* and *in vivo*, as well as the underlying mechanisms.

In this study, for the first time, we found that Rg5 at non-cytotoxic concentrations significantly potentiated the antitumor effects of chemotherapy agents including DOX, PTX, TXT, and DON to MDR cell lines A2780/T, and A549/T, but not affect the toxicity in sensitive cells. Moreover, Rg5 and TXT significantly inhibited the growth of drug resistance tumor by 48% in the A549/T xenograft model, which is comparable with the *in vivo* MDR effects reported

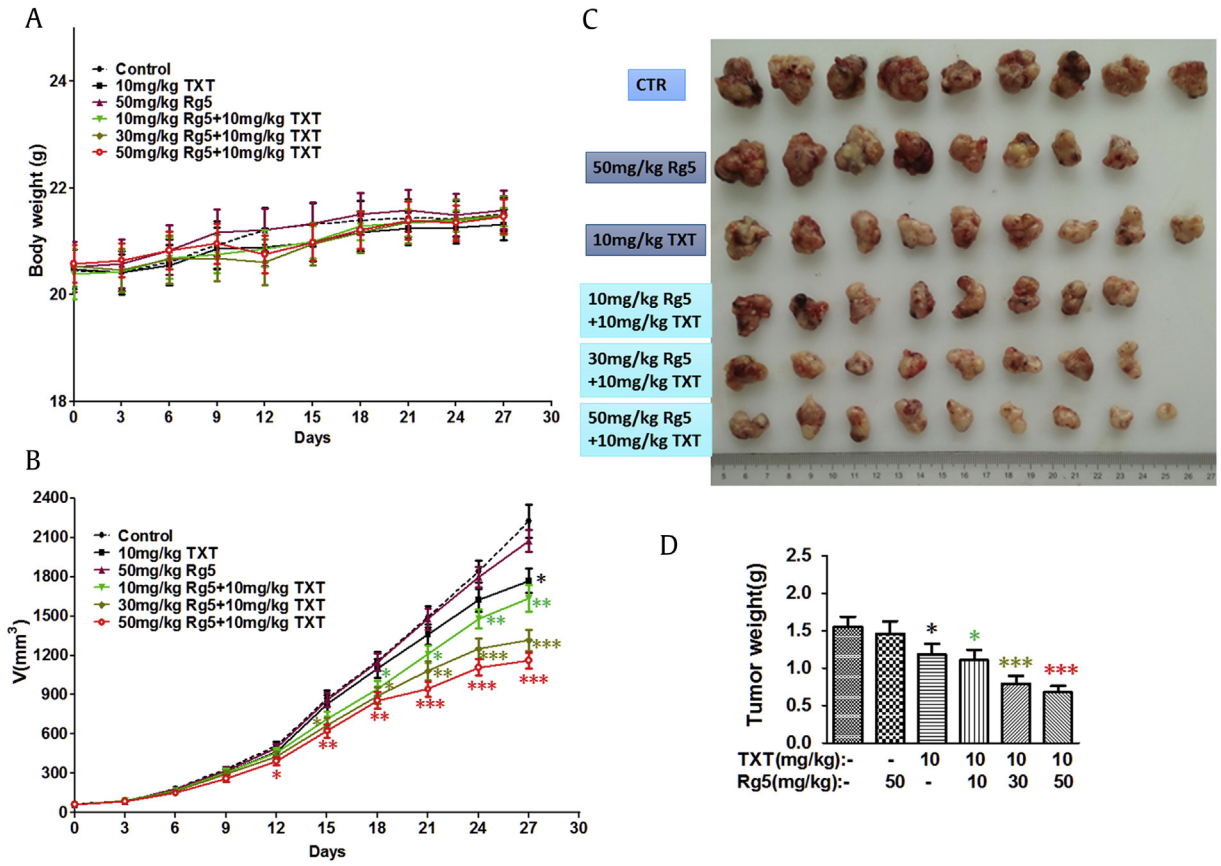

Fig. 8. Effects of treatment of Rg5 and docetaxel on A549/T cell xenograft nude mice model. (A) The body weight was drawn to monitor the body weight and tumor volume with time after implantation. (B) Tumour growth curves were drawn to monitor the body weight and tumor volume with time after implantation. The tumor xenografts were excised. (C) The tumors were photographed on the 27th day after implantation. (D) The tumors weighted on the 27th day after implantation. The data shown are expressed as the mean ± SD for each group (n = 9 or 10), $^{*}p < 0.05$, $^{**}p < 0.01$, $^{**}p < 0.001$.
CTR, control group given vehicle; SD, standard deviation; TXT, docetaxel.

in literature for the third generation P-gp inhibitors such as OC144-093 [38] and LY335979 [39]. The underlying mechanism study indicated that Rg5 inhibits the efflux activity of ABCB1 transporter leading to the intracellular accumulation of drugs in MDR cancer cells but not in sensitive cells, which was illustrated clearly by docking analysis as the ligand Rg5 was well-fitted into a druggable cavity of ABCB1 transporter with a similar affinity as QND.

As energy used by ABCB1 transporter comes from ATP hydrolysis, we also investigated the ATPase activity of ABCB1 transporter to confirm our previous assumption. Our results indicated that Rg5 might be a substrate of ABCB1 as it stimulated the activity of ATPase. Moreover, it inhibited the ATPase activity stimulated by Ver, indicating it bound to the ABCB1 transporter with high affinity and left little place for other agents bind to the transporter, which resulted in decreased activity of ABCB1 transporter.

Moreover, recent studies suggested that the MAPK/ERK, PI3K/AKT, and Nrf2 signaling pathways is important for multiple drugs resistance [28] as downregulating the AKT/ERK and Nrf2 signaling pathways could overcome MDR to drugs such as PTX, DOX, and 5-FU [30]. In this study, inhibition of AKT/ERK and Nrf2 pathways are associated with the sensitizing effect of Rg5. These results not only elucidate the multiple targets for the therapeutic effects of Rg5 but also was helpful for explaining the reversal effect of Rg5 against 5-FU which is not a P-gp substrate. Moreover, as Nrf2 expression could be induced via upregulation of PI3K/AKT and/or MAPK/ERK signaling pathways [40], the sensitizing effect of Rg5 to MDR could be caused by downregulating the PI3K-Akt pathways which reduced the Nrf2 expression.

Although Nrf2 has emerged as an important contributor to chemoresistance, how Nrf2 plays such a role still remains unknown. A growing amount of evidence indicates that Nrf2 transcription promotes ROS detoxification and carcinogenesis though metabolic rewiring to support the antioxidant systems, leading to cancer cell growth and proliferation [41–43]. In addition, Nrf2-mediated regulation of ABCC2 and ABCG2 expression confers chemoresistance via enhancing drug efflux [44,45]. Recently, overexpression of Nrf2 and ABCB1/P-gp were observed in colorectal cancer patients [46], and Nrf2 overexpression is associated with P-glycoprotein upregulation in gastric cancer [47] which is consistent with our observation in A2780/T cells and A549/T cells. However, in this study, Rg5 could downregulate Nrf2 signaling but not change P-gp protein level in A2780/T cells, indicating that inhibition of Nrf2 expression can improve the efficacy of chemotherapeutic agents in addition to inhibiting P-gp mediated drug efflux.

In conclusion, this study demonstrated that Rg5 effectively overcomes ABCB1-mediated drug resistance by inhibiting ABCB1 transporter and suppressing the chemoresistance-related AKT/Nrf2 pathways. In addition, Rg5 did not affect the expression of ABCB1 transporter. Considering the safety of Rg5, we believe that Rg5 may be a good combination therapy candidate for ABCB1-medicated drug resistance.

Conflicts of interest

All authors declare no conflict of interest.

Acknowledgments

This work was financially supported by the grant from Macao Science and Technology Development Fund, Macau Special Administrative Region (003/2017/A1 to Y. Xie.).

Appendix A. Supplementary data

Supplementary data to this article can be found online at https://doi.org/10.1016/j.jgr.2018.10.007.

References

[1] Alfarouk KO, Stock C-M, Taylor S, Walsh M, Muddathir AK, Verduzco D, Bashir AHH, Mohammed OY, Elhassan GO, Harguindey S, et al. Resistance to cancer chemotherapy: failure in drug response from ADME to P-gp. Cancer Cell Int 2015;15:71.
[2] Baguley BC. Multidrug resistance in cancer. Methods Mol Biol 2010;596:1–14.
[3] Gillet JP, Gottesman MM. Mechanisms of multidrug resistance in cancer. Methods Mol Biol 2010;596:47–76.
[4] Coley HM. Overcoming multidrug resistance in cancer: clinical studies of p-glycoprotein inhibitors. Methods Mol Biol 2010;596:341–58.
[5] Yu M, Ocana A, Tannock IF. Reversal of ATP-binding cassette drug transporter activity to modulate chemoresistance: why has it failed to provide clinical benefit? Cancer Metastasis Rev 2013 Jun;32(1–2):211–27.
[6] Wang J, Seebacher N, Shi H, Kan Q, Duan Z. Novel strategies to prevent the development of multidrug resistance (MDR) in cancer. Oncotarget 2017;8(48):84559–71.
[7] Ramos P, Bentires-Alj M. Mechanism-based cancer therapy: resistance to therapy, therapy for resistance. Oncogene 2015;34(28):3617–26.
[8] Dinic J, Podolski-Renic A, Stankovic T, Bankovic J, Pesic M. New approaches with natural product drugs for overcoming multidrug resistance in cancer. Curr Pharmaceut Des 2015;21(38):5589–604.
[9] Wu C-P, Ohnuma S, Ambudkar SV. Discovering natural product modulators to overcome multidrug resistance in cancer chemotherapy. Curr Pharmaceut Biotechnol 2011;12(4):609–20.
[10] Dennis T, Fanous M, Mousa S. Natural products for chemopreventive and adjunctive therapy in oncologic disease. Nutr Cancer 2009;61(5):587–97.
[11] Mir IA, Tiku AB. Chemopreventive and therapeutic potential of "naringenin," a flavanone present in citrus fruits. Nutr Cancer 2015;67(1):27–42.
[12] Zhou S, Lim LY, Chowbay B. Herbal modulation of P-glycoprotein. Drug Metabol Rev 2004 Feb;36(1):57–104.
[13] Zhang J, Zhou F, Niu F, Lu M, Wu X, Sun J, Wang G. Stereoselective regulations of P-glycoprotein by ginsenoside Rh2 epimers and the potential mechanisms from the view of pharmacokinetics. PLoS One 2012;7(4), e35768.
[14] Zhang J, Zhou F, Wu X, Zhang X, Chen Y, Zha BS, Niu F, Lu M, Hao G, Sun Y, et al. Cellular pharmacokinetic mechanisms of adriamycin resistance and its modulation by 20(S)-ginsenoside Rh2 in MCF-7/Adr cells. Br J Pharmacol 2012 Jan;165(1):120–34.
[15] Yang LQ, Wang B, Gan H, Fu ST, Zhu XX, Wu ZN, Zhan DW, Gu RL, Dou GF, Meng ZY. Enhanced oral bioavailability and anti-tumour effect of paclitaxel by 20(s)-ginsenoside Rg3 in vivo. Biopharmaceut Drug Dispos 2012 Nov;33(8):425–36.
[16] Bai L, Gao J, Wei F, Zhao J, Wang D, Wei J. Therapeutic potential of ginsenosides as an adjuvant treatment for diabetes. Front Pharmacol 2018;9:423.
[17] Kim JH, Yi YS, Kim MY, Cho JY. Role of ginsenosides, the main active components of Panax ginseng, in inflammatory responses and diseases. J Ginseng Res 2017 Oct;41(4):435–43.
[18] Lawler M, Alsina D, Adams RA, Anderson AS, Brown G, Fearnhead NS, Fenwick SW, Halloran SP. Critical research gaps and recommendations to inform research prioritisation for more effective prevention and improved outcomes in colorectal cancer. Gut 2018 Jan;67(1):179–93.
[19] van Tonder A, Joubert AM, Cromarty AD. Limitations of the 3-(4,5-dimethylthiazol-2-yl)-2,5-diphenyl-2H-tetrazolium bromide (MTT) assay when compared to three commonly used cell enumeration assays. BMC Res Notes 2015 Feb 20;8:47.
[20] Ma W, Feng S, Yao X, Yuan Z, Liu L, Xie Y. Nobiletin enhances the efficacy of chemotherapeutic agents in ABCB1 overexpression cancer cells. Sci Rep 2015 Dec 22;5:18789.
[21] Ashton JC. Drug combination studies and their synergy quantification using the Chou-Talalay method–letter. Cancer Res 2015 Jun 1;75(11):2400.
[22] Chou TC. Drug combination studies and their synergy quantification using the Chou-Talalay method. Cancer Res 2010 Jan 15;70(2):440–6.
[23] Yuan ZW, Li YZ, Liu ZQ, Feng SL, Zhou H, Liu CX, Liu L, Xie Y. Role of tangeretin as a potential bioavailability enhancer for silybin: pharmacokinetic and pharmacological studies. Pharmacol Res 2018 Feb;128:153–66.
[24] Coxon A, Ziegler B, Kaufman S, Xu M, Wang H, Weishuhn D, Schmidt J, Sweet H, Starnes C, Saffran D, et al. Antitumor activity of motesanib alone and in combination with cisplatin or docetaxel in multiple human non–small-cell lung cancer xenograft models. Mol Cancer 2012 September 19;11(1):70.
[25] Kim SJ, Kim AK. Anti-breast cancer activity of Fine Black ginseng (Panax ginseng Meyer) and ginsenoside Rg5. J Ginseng Res 2015 Apr;39(2):125–34.
[26] Lin X, Skolnik S, Chen X, Wang J. Attenuation of intestinal absorption by major efflux transporters: quantitative tools and strategies using a Caco-2 model. Drug Metab Dispos 2011 Feb;39(2):265–74.
[27] Rozengurt E, Soares HP, Sinnet-Smith J. Suppression of feedback loops mediated by PI3K/mTOR induces multiple overactivation of compensatory pathways: an unintended consequence leading to drug resistance. Mol Cancer Ther 2014 Nov;13(11):2477–88.
[28] Furfaro AL, Traverso N, Domenicotti C, Piras S, Moretta L, Marinari UM, Pronzato MA, Nitti M. The Nrf2/HO-1 axis in cancer cell growth and chemoresistance. Oxidative Med Cell Longev 2016;2016, 1958174.
[29] Jeddi F, Soozangar N, Sadeghi MR, Somi MH, Samadi N. Contradictory roles of Nrf2/Keap1 signaling pathway in cancer prevention/promotion and chemoresistance. DNA Repair 2017 Jun;54:13–21.
[30] McCubrey JA, Steelman LS, Chappell WH, Abrams SL, Franklin RA, Montalto G, Cervello M, Libra M, Candido S, Malaponte G, et al. Ras/Raf/MEK/ERK and PI3K/PTEN/Akt/mTOR cascade inhibitors: how mutations can result in therapy resistance and how to overcome resistance. Oncotarget 2012 Oct;3(10):1068–111.
[31] Gao A-M, Ke Z-P, Wang J-N, Yang J-Y, Chen S-Y, Chen H. Apigenin sensitizes doxorubicin-resistant hepatocellular carcinoma BEL-7402/ADM cells to doxorubicin via inhibiting PI3K/Akt/Nrf2 pathway. Carcinogenesis 2013;34(8):1806–14.
[32] Roh J-L, Kim EH, Jang H, Shin D. Nrf2 inhibition reverses the resistance of cisplatin-resistant head and neck cancer cells to artesunate-induced ferroptosis. Redox Biol 2017;11:254–62.
[33] Wang X-J, Sun Z, Villeneuve NF, Zhang S, Zhao F, Li Y, Chen W, Yi X, Zheng W, Wondrak GT, et al. Nrf2 enhances resistance of cancer cells to chemotherapeutic drugs, the dark side of Nrf2. Carcinogenesis 2008;29(6):1235–43.
[34] Qi W, Cooke LS, Liu X, Rimsza L, Roe DJ, Manziolli A, Persky DO, Miller TP, Mahadevan D. Aurora inhibitor MLN8237 in combination with docetaxel enhances apoptosis and anti-tumor activity in mantle cell lymphoma. Biochem Pharmacol 2011 Apr 1;81(7):881–90.
[35] Hejazi E, Nasrollahzadeh J, Fatemi R, Barzegar-Yar Mohamadi L, Saliminejad K, Amiri Z, Kimiagar M, Houshyari M, Tavakoli M, Idali F. Effects of combined soy isoflavone extract and docetaxel treatment on murine 4T1 breast tumor model. Avicenna J Med Biotechnol 2015 Jan-Mar;7(1):16–21.
[36] Li W, Yan MH, Liu Y, Liu Z, Wang Z, Chen C, Zhang J, Sun YS. Ginsenoside Rg5 ameliorates cisplatin-induced nephrotoxicity in mice through inhibition of inflammation, oxidative stress, and apoptosis. Nutrients 2016 Sep 13;8(9).
[37] Fan H, Xiao-ling S, Yaliu S, Ming-ming L, Xue F, Xian-sheng M, Li F. Comparative pharmacokinetics of ginsenoside Rg(3) and ginsenoside Rh(2) after oral administration of ginsenoside Rg(3) in normal and walker 256 tumor-bearing Rats. Phcog Mag 2016 Jan-Mar;12(45):21–4.
[38] Newman MJ, Rodarte JC, Benbatoul KD, Romano SJ, Zhang C, Krane S, Moran EJ, Uyeda RT, Dixon R, Guns ES, et al. Discovery and characterization of OC144-093, a novel inhibitor of P-glycoprotein-mediated multidrug resistance. Cancer Res 2000 Jun 01;60(11):2964–72.
[39] Dantzig AH, Shepard RL, Cao J, Law KL, Ehlhardt WJ, Baughman TM, Bumol TF, Starling JJ. Reversal of P-glycoprotein-mediated multidrug resistance by a potent cyclopropyldibenzosuberane modulator, LY335979. Cancer Res 1996 Sep 15;56(18):4171–9.
[40] Hewage SRKM, Piao MJ, Kang KA, Ryu YS, Fernando PMDJ, Oh MC, Park JE, Shilnikova K, Moon YJ, Shin DO, et al. Galangin activates the ERK/AKT-driven Nrf2 signaling pathway to increase the level of reduced glutathione in human keratinocytes. Biomol Ther 2017;25(4):427–33.
[41] Sayin VI, LeBoeuf SE, Singh SX, Davidson SM, Biancur D, Guzelhan BS, Alvarez SW, Wu WL, Karakousi TR, Zavitsanou AM, et al. Activation of the NRF2 antioxidant program generates an imbalance in central carbon metabolism in cancer. eLife 2017;6, e28083.
[42] Chio IIC, Jafarnejad SM, Ponz-Sarvise M, Park Y, Rivera K, Palm W, Wilson J, Sangar V, Hao Y, Ohlund D, et al. NRF2 promotes tumor maintenance by modulating mRNA translation in pancreatic cancer. Cell 2016 Aug 11;166(4):963–76.
[43] No JH, Kim YB, Song YS. Targeting nrf2 signaling to combat chemoresistance. J Cancer Prevent 2014 Jun;19(2):111–7.
[44] Chen Q, Li W, Wan Y, Xia X, Wu Q, Chen Y, Lai Z, Yu C, Li W. Amplified in breast cancer 1 enhances human cholangiocarcinoma growth and chemoresistance by simultaneous activation of Akt and Nrf2 pathways. Hepatology (Baltimore, Md) 2012 Jun;55(6):1820–9.
[45] Singh A, Wu H, Zhang P, Happel C, Ma J, Biswal S. Expression of ABCG2 (BCRP) is regulated by Nrf2 in cancer cells that confers side population and chemoresistance phenotype. Mol Cancer Ther 2010;9(8):2365–76.
[46] Sadeghi MR, Jeddi F, Soozangar N, Somi MH, Shirmohamadi M, Khaze V, Samadi N. Nrf2/P-glycoprotein axis is associated with clinicopathological characteristics in colorectal cancer. Biomed Pharmacother = Biomedecine & Pharmacotherapie 2018 Aug;104:458–64.
[47] Jeddi F, Soozangar N, Sadeghi MR, Somi MH, Shirmohamadi M, Eftekhar-Sadat AT, Samadi N. Nrf2 overexpression is associated with P-glycoprotein upregulation in gastric cancer. Biomed Pharmacother = Biomedecine & Pharmacotherapie 2018 Jan;97:286–92.